

Temperature dependence of the conductivity and kinetics of oxygen intercalation of C₇₀ films

Daxing Han

Department of Physics and Astronomy, University of North Carolina at Chapel Hill, Chapel Hill, North Carolina 27599-3255

Hitoe Habuchi

Gifu National College of Technology, Sinsei-cho, Motosugun, Gifu, 501-04, Japan

Shoji Nitta

Department of Electronic and Computer Engineering, Faculty of Engineering, Gifu University, 1-1 Yanaido, Gifu 501-11, Japan

(Received 1 August 1997)

Electrical conductivity values of 1.8×10^{-9} to 1.8×10^{-13} ($\Omega \text{ cm}$)⁻¹ at 30 °C were found in undoped C₇₀ films, and the conductivity is thermally activated with an activation energy of 0.51–0.81 eV and a pre-exponential factor of 0.5 ($\Omega \text{ cm}$)⁻¹. We demonstrated that the conductivity decay due to oxygen intercalation follows $\sigma(t) = \sigma(0)t^{-\alpha}$, where $\alpha \ll 1$ when $0 < t < t_1$, $\alpha \gg 1$ when $t_1 < t < t_2$, and $0.5 \leq \alpha < 1.0$ when $t > t_2$, corresponding to three processes of oxygen reaction with the film. [S0163-1829(98)01308-3]

I. INTRODUCTION

Both theoretical calculation and experimental investigation of the electrical conductivity have shown semiconducting behavior in C₆₀ and C₇₀ fullerenes.¹ The simplest picture is that the highest occupied molecular-orbital electronic state (h_u) forms the valence band, and the lowest unoccupied molecular orbital electronic state (t_{1u}) forms the conduction band. Experimentally, the room-temperature electrical resistivity was found to be $10^8 \Omega \text{ cm}$ for oxygen-free C₆₀ films,² and $10^{14} \Omega \text{ cm}$ for mixed C₆₀ and C₇₀ films after exposure to air.³ However, contradictory values of the energy levels of the defect states deduced from the conductivity activation energy have been reported.^{4,5} In oxygen-free single-crystal C₆₀, the conductivity activation energies were found to be 0.26 and 0.15 eV, and was described as an impurity level in Ref. 4. In a previous work, we found 0.51 eV for undoped oxygen-free mixtures of C₆₀ and C₇₀ films.⁵ Furthermore, reversible oxygen intercalation with solid C₆₀ and C₇₀ has been found by both electrical conductivity and molecular structure studies.^{2–6} To the best of our knowledge, the kinetics of oxygen intercalation in fullerenes has not been studied. In this paper we present interesting experimental results of the electrical conductivity of C₇₀ films, their activation energy, and the kinetics of oxygen intercalation, to gain insight into the electrical properties and the electronic structure of these fullerenes.

II. EXPERIMENT AND RESULTS

Polycrystalline C₇₀ powder (99% C₇₀ and 1% C₆₀) was preheated in a vacuum ($< 10^{-5}$ Torr) at 250 °C for 8 h to remove toluene and gases from the powder. The C₇₀ films were evaporated onto 7059 glass and quartz substrates for electrical and optical measurements, respectively. The source temperature was 450 °C, and the substrate temperature was 250 °C. The evaporation shutter was opened after 10 min of heating the source to 450 °C in order to get rid of the C₆₀ molecules in the source, so that only C₇₀ would be evapo-

rated onto the substrates. The thickness of the polycrystalline films was 2.14 μm , and the crystallite sizes were about 40 nm measured by x-ray diffraction.⁷ For conductivity studies, coplanar Al electrodes with a 60- μm gap and 3-mm length were evaporated onto the top of the film.

For these fullerene films, the optical absorption edge was measured by photothermal deflection spectroscopy,⁸ and the optical gap E_0 was determined by using the Tauc model of $\alpha(E)h\nu \propto (E - E_0)^2$, which is based on assumptions of a constant optical matrix element and a parabolic density of states.⁹ For the C₇₀ films, we found that the optical gap of 1.7–1.8 eV is larger than that of 1.6 eV for C₆₀.^{1,8} In order to verify the value of the optical gap, we measured photoluminescence (PL) spectra in a temperature range of 10–300 K for both C₆₀ and C₇₀ films.¹⁰ The energy position of the PL main peak was found to be 1.79 eV for C₇₀, and 1.69 eV for C₆₀ films. Again, the optical gap of the C₇₀ film is 0.1 eV larger than that of the C₆₀ film. Furthermore, the majority-carrier type of the C₇₀ solid was measured by using the thermoelectric power technique. After heat treatment at 200 °C in vacuum, the film was found to be n type.

The conductivity measurements were carried out in a 10^{-3} -Torr vacuum in the temperature range of 300–500 K without causing a change of the polycrystalline structure. A programmable temperature controller was used. The accuracy of the measurements of temperature and time was ± 0.05 °C and ± 1 s, respectively. The I - V characteristic was linear in the beginning of the measurements, then became nonlinear at low field ($\sim 10^3$ V/cm) after a few runs, perhaps due to the formation of a thin Al₂O₃ layer at the Al/C₇₀ interface. When we evaporated a thin layer of MgO between the Al and the fullerene film, the initial conductivity was larger than the case of Al alone, but the I - V characteristic became nonlinear again in low field ($\sim 10^3$ V/cm) after exposure of the sample in air. So we believe that the nonlinearity of the I - V curve at low field is an intrinsic problem of the fullerene films in oxygen-intercalated state. Nevertheless, the results were reproducible in the linear region of 1 – 6×10^4 V/cm.

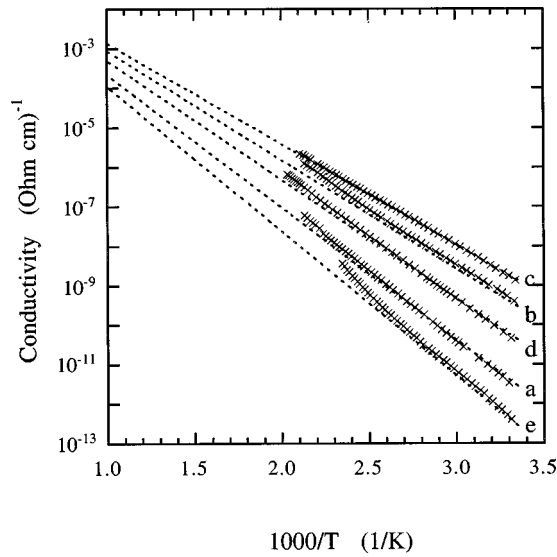


FIG. 1. Conductivity temperature dependence of a C_{70} film in vacuum at several stages (see text). The dashed lines are calculated data according to $\sigma = \sigma_0 \exp[-E_a/kT]$ where $\sigma_0 = 0.5$ ($\Omega \text{ cm}^{-1}$) and $E_a = 0.51, 0.55, 0.6, 0.67,$ and 0.73 eV, respectively.

Figure 1 shows five typical curves of the conductivity versus inverse temperature from one C_{70} film. They are (curve *a*) the first run of increasing temperature with a heating rate of $1^\circ\text{C}/\text{min}$; (curve *b*) after annealing at 200°C for 15 h, with decreasing temperature at $1^\circ\text{C}/\text{min}$ from 200 to 100°C , then natural cooling; (curve *c*) after annealing at 200°C for 93 h, with decreasing temperature in the same manner as (curve *b*); (curve *d*) after annealing 15 h at 220°C following exposure to air for 193 h at room temperature, at decreasing temperature with varied rate; and (curve *e*) at increasing temperature with varied rate after exposure to air for 25 h at 80°C . A temperature ramp rate of $1^\circ\text{C}/\text{min}$ was normally used, but with a varied rate from 0.1 to $5^\circ\text{C}/\text{min}$ the thermally activated behavior did not change below about 150°C . This implies that the annealing effect on electron transport does not occur below 150°C in most cases. One exception is curve *e*, in that the data were taken after exposing the film to air at 80°C ; the annealing effect then started at about 85°C . Regardless of the temperature increase or decrease, the conductivity always shows a thermally activated behavior in the C_{70} films:

$$\sigma = \sigma_0 \exp[-E_a/kT], \quad (1)$$

where σ_0 is the pre-exponential factor and E_a is the activation energy. In more than ten runs of heating and cooling cycles, $0.51 \text{ eV} < E_a < 0.81 \text{ eV}$ was observed. The smallest activation energy (0.51 eV) was found in the well-annealed state (curve *c*) while the largest activation energy (0.81 eV) was found in the air-exposed state (see Fig. 2). Inserting the measured value of E_a and using $\sigma_0 = 0.5 \Omega \text{ cm}^{-1}$, the calculated curves agree well with the experimental results below 150°C as shown in Fig. 1. The deviation of the experimental data from the law presented in Eq. (1) is due to the annealing effect. The room temperature conductivity as a function of the activation energy is summarized in Fig. 2. The dashed

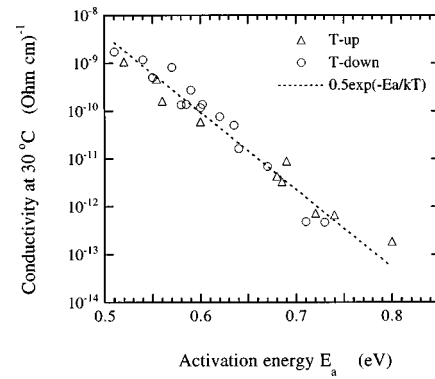


FIG. 2. The room-temperature conductivity as a function of the activation energy from the same C_{70} film as shown in Fig. 1.

line is the calculated curve according to Eq. (1), where $\sigma_0 = 0.5 \Omega \text{ cm}^{-1}$. Again, the calculated curve agrees with the experimental results at 30°C .

We further show the kinetics of both air and oxygen intercalation with the C_{70} film measured by the conductivity as a function of the exposure time. Figure 3 shows the decrease of the conductivity upon exposing the film to air and to 99.99% oxygen gas at room temperature, respectively. The similarity of the two curves in Fig. 3 implies that oxygen molecular intercalation is the dominant process in both conditions. The different values of the conductivity are due to the different stages of the film history. Figure 4 shows the decrease of the conductivity upon exposing the film to air at 80°C , where the C_{70} molecule is in the rotation-free phase.^{11,12} The data in Figs. 3 and 4 can be described by an exponential function as

$$\sigma(t) = \sigma(0)t^{-\alpha},$$

$$\alpha \ll 1 \quad \text{when } 0 < t < t_1 \quad (2)$$

$$\alpha \geq 1 \quad \text{when } t_1 < t < t_2$$

$$0.5 \leq \alpha < 1.0 \quad \text{when } t > t_2.$$

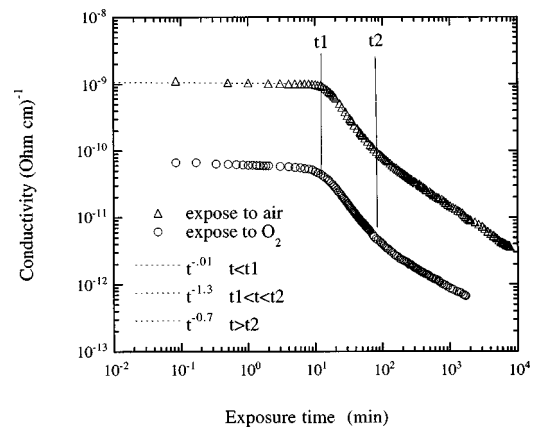


FIG. 3. The conductivity of the C_{70} film as a function of the exposure time to either air or oxygen gas at 28°C . The results from both measurements show three time regimes separated by t_1 and t_2 . The dashed line is calculated according to $\sigma(t) = \sigma(0)t^{-\alpha}$. The symbols for air and gas and the value of α are noted in the figure.

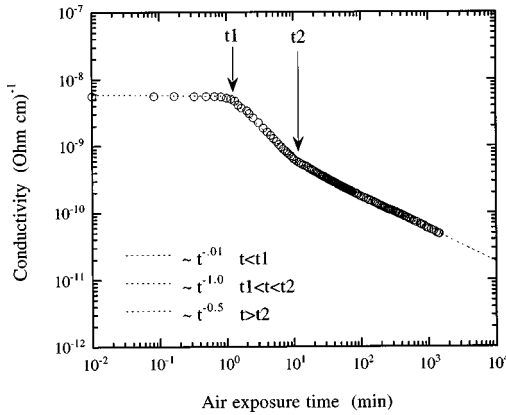


FIG. 4. Dependence of the conductivity of the C_{70} film on exposure time to air at 80 °C. The data show three time regimes separated by t_1 and t_2 . The dashed line is calculated according to $\sigma(t) = \sigma(0)t^{-\alpha}$, and the values of α are noted.

The three regimes of the conductivity decrease suggest three processes of molecular oxygen intercalation with the C_{70} film: (a) slow, (b) fast, and (c) intermediate. In this work, it took a few seconds to switch the sample chamber from vacuum to ambient pressure. Hence the slow process can not be due to the time required for the gas to flow into the sample chamber.^{16–18}

In order to change the film from an oxygen-intercalated to an oxygen-free state, desorption of the oxygen from the film by annealing at 200 °C in vacuum is needed. We show one typical annealing process in the following. Right after the measurements of curve e in Fig. 1, the temperature was continually increased up to 200 °C. The annealing effect was recorded at 200 °C by the time dependence of the conductivity as shown in Fig. 5. One finds three steps in the annealing processes: a minor annealing effect in the first ten minutes, followed by a major annealing effect, which finally saturates after about 10 h. It is worthwhile to mention here that in the temperature range of these measurements, the film can reach a uniform temperature within 0.1 min. Therefore, the minor annealing step cannot be a thermal delay effect. In addition we have recorded the conductivity annealing processes from an oxygen-intercalated to an oxygen-free state at temperatures of 200, 230, and 250 °C. The same three-step features as in Fig. 5 were found. One possible explanation of the minor annealing process is the desorption of the oxygen molecule from the large area of the polycrystalline surfaces and

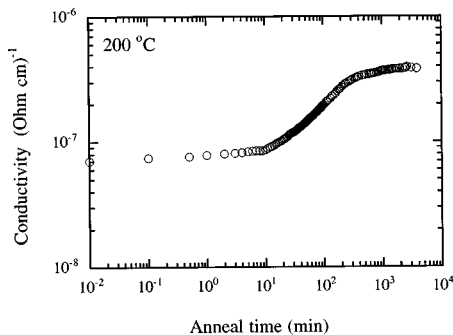


FIG. 5. The oxygen desorption processes at 200 °C annealing in a vacuum of 10^{-3} Torr for the C_{70} film after exposure to air at 80 °C.

the outer surfaces of the C_{70} molecule. During this surface-desorption process the molecular structure and the conductivity are not changed significantly. Following the surface-oxygen desorption, the decrease of the oxygen-related-defect states by breaking the carbon-oxygen bonds takes place during the major annealing process. Consequently, the conductivity increases until it reaches a saturation value. The films annealed at 230 and 250 °C showed no activation energy smaller than 0.51 eV. The minimum density of oxygen-related-defect states in this study perhaps is limited by the vacuum of 10^{-3} Torr. We have chosen 200 °C, 10 h as standard conditions for annealing the film to the oxygen-free state. At the moment, we do not know whether the defect density and/or the activation energy would be lower in an ultrahigh vacuum.

III. SUMMARY AND DISCUSSION

As seen above, we found that unlike the rapid increase of the conductivity in the first heating run in the C_{60} film,⁴ the conductivity of the C_{70} film is always thermally activated. This implies the C_{70} film is more stable than the C_{60} film in atmosphere. This can be explained by (a) the higher oxygen intercalation energy barrier of the C_{70} than the C_{60} molecule,⁶ and (b) that the annealing effect does not occur until 150 °C. Based on one-electron arguments, the results in Fig. 1 demonstrate that the Fermi level E_F lies below E_c in the defect states. Equation (1) shows that trapped electrons near the Fermi level are thermally excited to the conduction band, which results in a thermally activated conductivity, and the thermal activation energy $E_a = E_c - E_F$. The observed E_a value of 0.51–0.81 eV implies that the oxygen-related defect state moves the Fermi-level position down to the middle of the gap. A pre-exponential factor of the conductivity is found to be $\sigma_0 = 0.5 \Omega \text{ cm}^{-1}$. The value of σ_0 in the C_{70} film is 1–2 orders of magnitude lower than that in noncrystalline and doped crystalline semiconductors.^{13,14}

The reversible change of the resistivity in single-crystal C_{60} has been described by oxygen desorption and absorption effects.⁴ It has been found⁶ that the molecular oxygen intercalates with C_{60} and C_{70} in a similar way, irrespective of their different molecular structure. This is perhaps due to the fact that the nonplanar sp^2 bands in both C_{60} and C_{70} are a more important factor in the initial stages of oxidation than is the shape of the fullerene molecule. The conductivity decreases as a function of the oxygen reaction time, $\sigma(t) = \sigma(0)t^{-\alpha}$, where α is the decay rate. Furthermore, three processes of oxygen reaction with the C_{70} films were demonstrated: (a) When $0 < t < t_1$, the slow process is dominant by the adsorption of the oxygen molecules on the polycrystalline surfaces and the outer surfaces of the C_{70} molecules. One possibility is that the molecular oxygen fills octahedral voids.^{15,16} Thus the fullerene molecular structure has not yet been modified, and there are no significant changes in the conductivity. Because of the relatively large area of those surfaces, this process takes a time period of the order of minutes. It is reasonable that this period would be longer at room temperature (about 10 min as shown in Fig. 3) and shorter at higher temperature (1 min. at 80 °C in Fig. 4). In the latter case, the C_{70} molecule is in the rotation-free phase,^{11,12} therefore, a short oxygen adsorption process due

to the increase of the diffusion coefficient is expected. (b) When $t_1 < t < t_2$, the fast decay of the conductivity can be explained by oxygen molecules intercalating between the C_{70} molecules, which creates acceptor states and moves the Fermi level to the middle of the gap. Interestingly, $\alpha=1$ at 80 °C where the material is in the molecular orientation free-rotation phase. $\sigma(t) \propto t^{-1}$ can be deduced from a rate equation with a single set of a defect states, which implies that the oxygen intercalation creates one type of deep state in the C_{70} film. At room temperature the conductivity decay rate was even faster than at 80 °C ($\alpha=1.3$). One possible explanation is that the lowering of the symmetry of the C_{70} molecules in the orientation-disordered phase enhances the intercalation of the oxygen molecules. When $t > t_2$, the mild decay of the conductivity may be due to creating acceptor states energetically or spatially different from those in the fast decay process, for instance, electronic states related to C_{70} monoxide and dioxide. No saturation was reached during the measurement time period. We knew¹⁵ that the subgap optical absorption increases with prolonged exposure of the film to air, and thus the decrease of the conductivity is more likely due to an increase of an oxygen-related defect which acts as an acceptor and moves the Fermi-level position down to the middle of the gap. The intrinsic electronic band has not been affected by the oxygen effect.^{6,15}

A reversible change from an oxygen-intercalated state to an oxygen-free state can be done by annealing the film at

200 °C in a vacuum for 10 h. For the fullerene films, both the oxygen-adsorption and -desorption processes on the large area surfaces last several minutes before changes occur in the molecular and electronic structures. The annealing effect, which takes the film from an oxygen-intercalated to an oxygen-free state, was found to start from 150 °C when the oxygen intercalation occurred at room temperature; but the annealing effect started at lower temperature for the film after oxygen intercalation at 80 °C. It seems that some of the oxygen-related defect states created at higher temperature are easier to anneal out. The reason remains unclear.

In addition, we found that the C_{70} film is an *n*-type semiconductor. The majority carrier is therefore the electron, as in the C_{60} film.¹ For the C_{70} films the optical gap deduced from the optical-absorption edge and from the PL main peak is about 0.1 eV larger than the optical gap of C_{60} . This may be due to a higher binding energy per C atom in C_{70} relative to C_{60} .¹

ACKNOWLEDGMENTS

D. H. was supported by NSF Grant No. INT-9600229. She is grateful to K. Satoshi for his help with electrode preparation. The authors are grateful to I. Toshimasa for thermopower measurements. We would like to thank T. Itoh and T. Gotoh for many helpful discussions, and L. E. McNeil for helpful discussions and for her help with English.

¹M. S. Dresselhaus, G. Dresselhaus, and P. C. Eklund, in *Science of Fullerenes and Carbon Nanotubes* (Academic, San Diego, 1996), Chaps. 12 and 14.

²F. Stepniak, P. J. Benning, D. M. Poirier, and J. H. Weaver, *Phys. Rev. B* **48**, 1899 (1993).

³J. Mort, R. Ziolo, M. Machonkin, D. R. Huffman, and M. I. Ferguson, *Chem. Phys. Lett.* **186**, 284 (1991).

⁴T. Arai, Y. Murakami, H. Suematsu, K. Kikuchi, Y. Achiba, and I. Ikemoto, *Solid State Commun.* **8**, 827 (1992).

⁵H. Habuchi, S. Nitta, T. Nishiwaki, T. Itoh, S. Hasegawa, and S. Nonomura (unpublished).

⁶M. Wohlers, A. Bauer, Th. Rühle, F. Neitzel, H. Werner, and R. Schlogl, *Fullerene Sci. Technol.* **5**, 49 (1997).

⁷T. Itoh, S. Nitta, and S. Nonomura, *Appl. Surf. Sci.* **113/114**, 282 (1997).

⁸S. Hasegawa, T. Nishiwaki, H. Habuchi, S. Nitta, and S. Nonomura, *Fullerene Sci. Technol.* **3**, 163 (1995).

⁹G. D. Cody, *The Optical Absorption Edge of a-Si:H*, edited by J.

L. Pankove, *Semiconductors and Semimetals Vol. 21B* (Academic, New York, 1984).

¹⁰H. Habuchi, E. Nishimura, S. Nitta, and S. Nonomura, *Fullerene Sci. Technol.* **5**, 231 (1997); H. Habuchi, D. Han, S. Nitta, T. Itoh, T. Gotoh, and S. Nonomura (unpublished).

¹¹X. Knupfer, D. M. Poirier, and J. H. Weaver, *Phys. Rev. B* **49**, 2281 (1994).

¹²E. Grivei, B. Nysten, M. Cassart, and J-P. Issi, *Phys. Rev. B* **47**, 1705 (1993).

¹³N. F. Mott and E. A. Davis, *Electronic Processes in Non-Crystalline Materials*, 2nd ed. (Oxford University Press, Oxford, 1979).

¹⁴T. F. Rosenbaum, K. Andres, G. A. Thomas, and R. N. Bhatt, *Phys. Rev. Lett.* **45**, 1723 (1980).

¹⁵H. D. Beckhaus, S. Verevkin, C. Ruchardf, F. Diederich, C. Thilgen, H. U. ter Meer, H. Mohn, and W. Muller, *Angew. Chem.* **106**, 1033 (1994).

¹⁶R. A. Assink, J. E. Schirber, D. A. Loy, B. Morosin, and G. A. Carson, *J. Mater. Res.* **7**, 2136 (1992).